Rubber-Elasticity of Hybrid Organic–Inorganic Composites Evaluated Using Dynamic Mechanical Spectroscopy and Equilibrium Swelling

THOMAS M. MILLER, LICHENG ZHAO, ANTHONY B. BRENNAN

Department of Materials Science and Engineering, University of Florida, Gainesville, FL 32611

Received 19 June 1997; accepted 7 October 1997

ABSTRACT: Estimations of the average molar mass between crosslinks for sol-gel-derived poly(tetramethylene oxide) (PTMO)–polysilicate hybrid composites have been made using both dynamic tensile modulus and equilibrium swelling techniques. Modulus-based calculations have been performed using storage modulus values obtained from dynamic mechanical spectroscopy at frequencies ranging from 0.1 to 10 Hz. The analysis revealed that gels containing either 4 or 19% polysilicate (by volume) had an average molar mass between crosslinks significantly less than that predicted by a PTMO and SiO_2 rule of mixtures. Thus, the analysis indicates that there is extensive restriction of PTMO chain mobility in these gels. Aging of the 19% polysilicate-loaded gels in a basic ethylamine and water solution for 25 h, which has previously been shown to enhance phase separation without loss of optical transparency, results in increasing average chain length. To verify this approach, the values obtained using the dynamic mechanical spectroscopy-based technique were compared with those calculated using the Flory-Rehner equation. Somewhat surprisingly, the analyses by both techniques were in excellent agreement, thereby suggesting that, in the absence of chemical change, elementary rubber elasticity theory is a good tool for investigating the phase interactions in these seemingly nonideal hybrid composites. J Appl Polym Sci 68: 947–957, 1998

Key words: hybrid organic–inorganic composites; sol-gel processing; dynamic mechanical spectroscopy; rubber-elasticity theory; average molar mass between crosslinks

INTRODUCTION

Hybrid organic–inorganic composites are an exciting class of materials exhibiting synergistic mechanical and thermomechanical responses arising from the near molecular level of mixing present within the materials. Many materials and synthetic routes have been used in the production of hybrid composites, with the end-use dictating the selection of the organic phase and the processing route.[1,2] Examples of polymers that have been used in the synthesis of hybrid composites include poly(dimethylsiloxane,[3–6] tetramethylene oxide,[7–9] arylene ether ketone,[10] imide,[11] amide,[12,13] butadiene,[6] *p*-phenylene vinylene,[14] acrylate[15–20]), as well as epoxy[21] and commercially available Nafion® membranes.[22] Similarly, a variety of inorganic precursors have been studied, including metal alkoxides of aluminum, titanium, and zirconium, as well as novel reinforcing phases, such as layered silicate minerals.[7,23] The broad range of compositions of these materials have led to a number of commercial developments in the area of high-performance composites. In addition, numerous patents have been

Correspondence to: A. B. Brennan.

Contract grant sponsor: National Institute of Health; contract grant number: DEO 9307-07; contract grant sponsor: du Pont.

Journal of Applied Polymer Science, Vol. 68, 947–957 (1998)
 CCC 0021-8995/98/060947-11

issued for this class of materials.[24–26] We envision that the study of these materials will enable other use of these systems for specialized coatings and optical devices. Efforts in our laboratories have focused on the uses of hybrids derived from the simultaneous sol-gel processing of triethoxysilane endcapped poly(tetramethylene oxide) (PTMO) and the inorganic precursor for silica, tetraethoxysilane (TEOS). Our primary interest is the effect of the interphase on the mechanical and physical properties of these systems. To this end, we have previously investigated modifications to both the organic and inorganic phases with the goal of understanding the structure/property relations of these near homogeneous composites.[27–29]

With regard to modifications of the inorganic polysilicate phase, our results reveal that gels derived from an acid-catalyzed mixture of 60% (w/w) PTMO and 40% TEOS—which were subsequently swollen in a basic, 70% ethylamine in water solution for up to 24 h—exhibit enhanced phase separation of the PTMO and polysilicate phases.[27] This enhancement was not accompanied by a loss of optical transparency. In addition, changes in dynamic mechanical response were observed in that the thermally induced syneresis typically exhibited by these polysilicate crosslinked composites could be eliminated by aging the gels in the basic solution. These results, as well as infrared evidence to be presented shortly, suggest that during the first hour of exposure the ethylamine treatment is the chemical analog of a thermal cure in that exposure to the basic solution for 1 h drives the condensation reaction to virtual completion. Beyond the first hour, however, increased phase separation is observed in the dynamic mechanical spectroscopy (DMS) data as evidenced by the onset of PTMO crystallization. Such crystallization would occur only when the PTMO chains are set free of significant interactions with the vitreous polysilicate chains and thereby gain the mobility necessary to crystallize. We have proposed that this phase separation, which does not occur on the macro-optical scale, occurs via a simultaneous dissolution and reprecipitation process. This process is analogous to the ripening observed in "pure" silicates exposed to basic conditions.[30] In an attempt to quantify the changes induced by this polysilicate ripening on the network structure of the hybrid composite we have applied elementary rubber elasticity theory in conjunction with DMS. It will be shown that this somewhat unorthodox approach not only provides valuable qualitative insights into the interactions present within these near molecularly mixed composites, but also that there is excellent quantitative agreement with values calculated from equilibrium swelling.

Rubber elasticity theory should serve as a useful tool for quantifying the reduced elasticity of the PTMO chains in that interpenetration of polysilicate and PTMO chains should lead to entanglements or labile crosslinks that reduce the average molar mass between crosslinks, $\bar{M}_c$. Consequently, the more interactive or mixed that the phases are, the lower that the average chain length should be. The exceptional linearity of the DMS storage modulus versus temperature plots, to be shown shortly, suggest that the data could be used to calculate $\bar{M}_c$ based on the thermodynamic derivation of the elasticity relation[31]

$$G = \bar{N}_v kT = \frac{\rho RT}{\bar{M}_c} \tag{1}$$

where G is the shear modulus; $\bar{N}_v$ is the average number of covalently bonded, elastically active network chains per unit volume; k is the Boltzmann constant; R is the gas constant; T is absolute temperature; ρ is the density; and $\bar{M}_c$ is the average molar mass between crosslink junctions. If the sample is assumed to have a Poisson ratio, υ, of 0.5 throughout the temperature range of interest, then the elastic modulus, E, which is related to the shear modulus by the equation

$$E = 2G(1 + \upsilon) \tag{2}$$

is equal to $3G$. In addition, if the characteristic relaxation time of the gel is less than the timescale of the dynamic modulus measurement, then the storage modulus, E', is effectively an equilibrium measurement equivalent to the equilibrium elastic modulus, E. Equation (1) can then be updated to the form

$$E' = 3\bar{N}_v kT = \frac{3\rho RT}{\bar{M}_c} \tag{3}$$

Examination of this equation reveals that a linear regression through a plot of E' versus 3 kT yields a slope of $\bar{N}_v$ and a crosslink density of $\bar{N}_v/2$, assuming tetrafunctional crosslink junctions. Equating the second and third expressions of the equalities in eq. (3) produces the relation

$$\bar{M}_c = \frac{\rho L}{\bar{N}_v} \quad (4)$$

where L is the Avogadro constant and, again, ρ is the density of the gel. It is evident that the assumption of a tetrafunctional crosslink junction in this complex mixture is a bit of a stretch from the classical concept. However, one must recognize that the system is a mixture of tetrafunctional cross link junctions with regard to the TEOS and trifunctional with regard to the PTMO oligomers. Furthermore, the actual structure of the silicate phase would most likely have an average functionality much higher than the individual structural repeat units. The relative reactivity of these species and the overall extent of reaction is not well defined; however, the results of our, as yet to be shown analysis, indicate that the average functionality of the system can be approximated by the value of 4.

A check on the values obtained using eq. (4) can be made using the more traditional equilibrium swelling technique in conjunction with the Flory-Rehner equation for a perfect network,[32,33]

$$-[(1 - v_{2m}) + v_{2m} + \chi_{1,2} v_{2m}^2] = \frac{V_1 \rho}{\bar{M}_c}\left(v_{2m}^{1/3} - \frac{v_{2m}}{2}\right) \quad (5)$$

where v_{2m} is the volume fraction of polymer in the equilibrium swollen mass, V_1 is the molar volume of the solvent, and $\chi_{1,2}$ is the Flory-Huggins interaction parameter. The volume fraction of the polymer in the swollen mass can be calculated using

$$v_{2m} = \frac{V_2}{V_1 + V_2} = \frac{M_2/\rho_2}{M_1/\rho_1 + M_2/\rho_2} \quad (6)$$

where V, M, and ρ are the volume, mass, and density, respectively; and the subscripts 1 and 2 correspond to the solvent and polymer, respectively. Note that the values estimated using this swelling technique have not been corrected for the volume fraction of polysilicate present [i.e., v_{2m} is based on volume fraction of solids in the swollen mass determined during extraction of the gels in tetrahydrofuran (THF), a good solvent].

The χ-parameter needed for determination using swelling can be estimated from the difference in solubility parameters of the gel and solvent using[34]

$$\chi_{1,2} = \frac{V_1}{RT}(\delta_1 - \delta_2)^2 \quad (7)$$

where, again, the subscripts 1 and 2 denote the solvent and hybrid gel, respectively. The value of δ_2 for the benchmark 40% (w/w) TEOS-based gel containing 19% polysilicate by volume was measured previously by equilibrium swelling studies of the gel in solvents of different Hildebrand parameters.[28] For this article, this same value was used for all the ethylamine exposure times, thereby assuming that swelling in the ethylamine solution produces no change in the Hildebrand parameter of the 40% TEOS hybrid gel. It is, of course, recognized that there are changes occurring in the silicate structure during the soaking of the gels in the ethylamine solution. However, those changes are limited largely to the silicate structure that exhibits relatively insignificant solvent uptake.[11]

These relations, having been developed under the stated assumptions, permit both a mechanical elasticity based and an equilibrium swelling based estimation of $\bar{M}_c$ for the PTMO chains present within the polysilicate crosslinked gels. It is, therefore, possible to compare the values obtained using the two approaches with insights gained into the effectiveness of DMS as a basis for such measurements. Second, it will be possible to use the measured values to quantify the extent of interaction, as evidenced by the change in average PTMO chain molar mass, between the organic and inorganic phases present in these hybrids.

Experimental

Details regarding the synthesis of the gels used in this article have been published previously along with complete mechanical and dynamic mechanical characterization results.[27] Consequently, the experimental techniques and testing parameters described therein pertain to this article also. Briefly, however, a dissolved mixture of 60%–40% (w/w) PTMO–TEOS, respectively, henceforth referred to as TEOS(40), were cast into polystyrene Petri dishes from an acidified isopropyl alcohol–THF (4 : 1) cosolvent system. The PTMO oligomers used in this study had been functionalized by reacting isocyanatopropyltriethoxysilane with 2000 g mol^{-1} poly(tetramethylene ether) glycol in bulk at 70°C for 4 days to produce reactive oligomers capable of undergoing sol-gel processing in the presence of additional metal alkox-

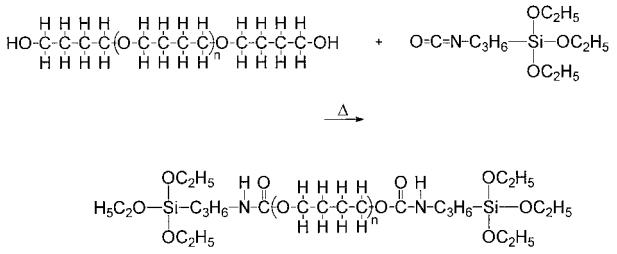

Figure 1 Mild heating of a 2% molar excess of isocyanatopropyltriethoxysilane mixed with 2000 g mol^{-1} poly(tetramethylene ether) glycol results in the formation of ethoxysilane-functionalized PTMO oligomers used in the sol-gel processing of all of the hybrid gels discussed in this study.

ides, such as TEOS. This reaction and the resulting end-capped oligomer are shown in Figure 1. After casting, the gels were covered and allowed to gel for 4 days. Subsequently, the gels were uncovered for 2 days to allow evaporation of any residual alcohol, water, or THF. Next, the gels were immersed in THF and allowed to swell at ambient for 24 h. This swelling was followed in series by vacuum-drying at 40°C and 29 in Hg for 24 h, swelling again in water at ambient for 24 h and a final vacuum-drying at 40°C and 29 in Hg for 24 h. After this processing, the gels were considered benchmarks and were ready for modification using the 70% ethylamine in water solution.

The standardized PTMO–polysilicate gels were placed into Pyrex Petri dishes prefilled with the aqueous ethylamine solution (pH 12.5) for 1, 4, 7, 13, and 25 h, after which they were removed and deswollen in water with multiple rinses until the pH of the deswelling water had returned to its initial value of 6.5 (ca. 8 h). Vacuum-drying under the conditions described previously completed the ethylamine processing.

For the sake of comparison, gels were made by crosslinking the PTMO chains without adding TEOS. These gels are referred to as TEOS(0) gels. The sol-gel processing of these reactive oligomers in the absence of TEOS produced an elasomeric gel containing ca. 4% polysilicate by volume. This gel underwent the same swelling/extraction and vacuum-drying process as the TEOS(40) gels.

Multiple characterization techniques were used for this study. DMS was performed using a Seiko DMS 200(FT) interfaced with a Seiko Rheostation model SDM/5600H. Testing for all gels was conducted from −150 to 200°C at a heating rate of 0.75°C min^{-1} in a dry nitrogen atmosphere maintained at an approximate flow rate of 200 mL min^{-1}. The test frequencies ranged from 0.1 to 10 Hz, whereas the strain amplitude was 0.1%.

Thermogravimetric analysis was performed using a Seiko TG/DTA 320 interfaced with the same Seiko Rheostation model SDM/5600H as the DMS 200(FT). A heating rate of 10°C min^{-1} in a dry air atmosphere maintained at a flow rate of approximately 100 mL min^{-1} was used. The temperature range investigated was 25 to 1000°C.

Swelling measurements were obtained by immersing three 9.5 mm diameter disks, which had been punched from the cast films using a no. 6 cork-borer, into small Petri dishes filled with THF. The averages and standard deviations given throughout this article are based on the swelling values for these three samples.

Density measurements were obtained using a Mettler density determination kit employing distilled water at ambient conditions. Five samples were used for each ethylamine exposure time, with the averages and standard deviations displayed in all figures.

Fourier-transform infrared (FTIR) spectroscopy was performed using a Nicolet 20SXB FTIR spectrometer. A Perkin-Elmer attenuated total reflection (ATR) stage was set to 45° using a KRS-5 trapezoidal crystal obtained from Spectra-Tech, Inc. In all cases, 32 scans were sufficient to collect reproducible spectra with an instrumental resolution of 4 cm^{-1}. All spectral subtractions were performed automatically using the OMNIC FT-IR software package supplied by Nicolet.

RESULTS

Physical Characteristics

The density and percent residue on ignition of the benchmark TEOS(0) and TEOS(40) gels, as well as the TEOS(40) gels exposed to the ethylamine and water solution for up to 25 h, are given in Table I. Examination of this data reveals that, as expected, the density of the gels and the percent residue on ignition increase as the mass loading of TEOS increases from 0 to 40% of the initial sol. Similarly, there is another slight increase in the residue mass for the 40% samples exposed to the ethylamine for 1 h. The density, however, decreases somewhat after the first hour of exposure. Changes such as these are possible if the number of structural defects, such as the hydroxyl groups known to be present in the polysilicate domains, are converted to oxygen bridges during the initial

Table I Room Temperature Densities of All Gels Investigated

Gel Type	Density @ 25°C (g cm^{-3})	% Residue on Ignition to 1000°C (10°C min^{-1}, air flow at 100 ml min^{-1})
TEOS(0) benchmark	1.028 ± 0.003	2.5
TEOS(40) benchmark	1.154 ± 0.002	20.5, 20.7
TEOS(40) 1-h exposure	1.146 ± 0.002	21.2, 21.1
TEOS(40) 4-h exposure	1.145 ± 0.003	21.0, 21.0
TEOS(40) 13-h exposure	1.147 ± 0.002	20.9, 20.8
TEOS(40) 25-h exposure	1.143 ± 0.002	20.8, 21.0

swelling stages, thereby producing a more highly connected polysilicate phase containing fewer volatiles.[35] A strong base, such as the ethylamine solution used in this study, would be an effective catalyst for such rapid refinements in the polysilicate phase and FTIR results presented next confirm these changes. However, for the gel density to decrease upon exposure to the ethylamine solution a volume expansion within the PTMO phase must occur to offset the increased polysilicate phase density. Results are presented in the following sections to explain this trend. Of critical importance, however, is that beyond the first hour of exposure of the gels to the basic solution, there seems to be no significant change in either gel density or mass residue on ignition. Similarly, this exposure does not result in any detectable loss of polysilicate in the bulk gels.

ATR FTIR Spectroscopy

In addition to verifying the hypothesis of silica refinement via enhanced condensation of unreacted hydroxyl groups during the first hour of exposure, an analysis of the polysilicate structures present is necessary to confirm that, beyond this first hour of exposure, no chemical changes leading to an increase in crosslink density occurred. Such changes would artificially increase the slope of the modulus versus temperature plots within the rubbery regimes of these gels. FTIR provides the insight needed to examine these chemical changes. However, the thickness of the hybrids, ca. 0.3 mm, negates the use of transmission FTIR. Therefore, the ATR technique was used on all gels.

The contributions of the polysilicate phase in all of these hybrids can be observed in two regions. Figure 2 displays the lower wavenumber region, or fingerprint region, dominated by the stretching of the ether linkages in the PTMO at 1100 cm^{-1}, the asymmetric stretching of the Si—O—Si groups at 1050 cm^{-1} and the Si—OH stretch at 955 cm^{-1}.[36–38] In addition, more subtle silicate-based absorbance is observable in the symmetric stretching/bending of Si—O—Si at ca. 800 cm^{-1} and what has been attributed to skeletal motion of 4-fold siloxane ring structures at ca. 570 cm^{-1}.[36,37,39] The second, or high wavenumber region, as shown in Figure 3, illustrates stretching bands for absorbed water and free Si—OH at ca. 3300 cm^{-1}.

Considering the spectra shown in Figure 2, the most pronounced change in the spectra induced by continued exposure to the ethylamine solution is that of the decreasing intensity of the asymmetric Si—O—Si stretching and Si—OH stretching. By taking the ratio of the $\upsilon_{\mathrm{Asym(Si—O—Si)}}$ to the $\upsilon_{\mathrm{C—O—C}}$ peak, shown as the lower plot in Figure 4, it is clear that there is a continued decrease in the strength of the Si—O—Si band with increasing exposure. The depth of penetration of an infra-

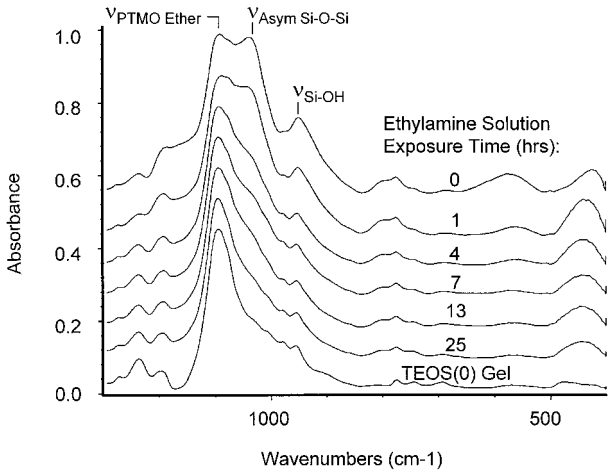

Figure 2 Low wavenumber region of the ATR-FTIR spectra of a benchmark TEOS(0) gel, benchmark TEOS(40) gel and TEOS(40) gels exposed to the ethylamine water solution for the indicated times.

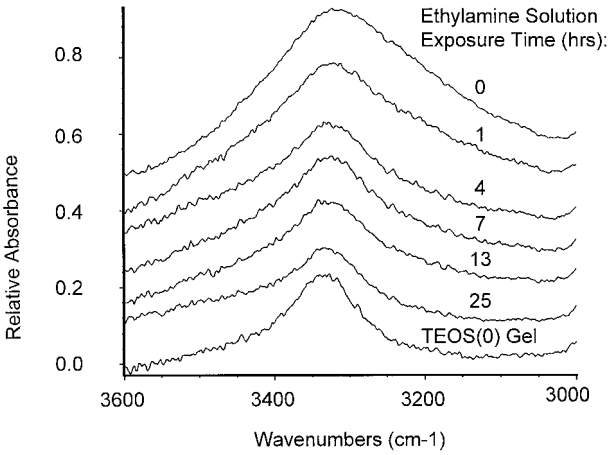

Figure 3 High wavenumber region of the ATR-FTIR spectra of a benchmark TEOS(0) gel, benchmark TEOS(40) gel, and TEOS(40) gels exposed to the ethylamine water solution for the indicated times.

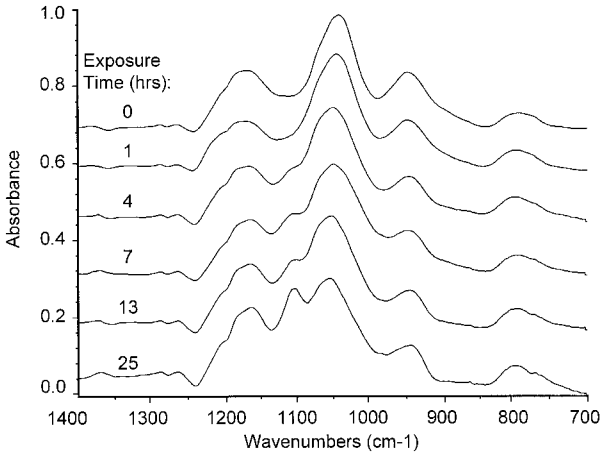

Figure 5 Low wavenumber region of the ATR-FTIR spectra of the TEOS(40) gels exposed to the ethylamine water solution for the indicated times after subtracting out the benchmark TEOS(0) spectra. The spectra, therefore, are those of the polysilicate phases in the TEOS(40) hybrids.

red beam is a function of wavelength, angle of incidence and the index of refraction of the material and crystal.[40] Based on these variables, the outermost 2 μm of the sample surface, or ca. 0.7% of total thickness, is being probed at 1050 cm^{-1}. This indicates that there is a reduction in the amount of polysilicate being detected near the surface of the gels after 24-h exposure. The thermal gravimetric analysis data presented in Table I, however, confirm that this reduction is negligible and that the overall amount of silica is virtually unchanged.

The issue that remains is what changes are the ethylamine solution inducing in the polysilicate phase that remains behind? This question can be answered by subtracting out the contribution of the crosslinked PTMO (i.e., the benchmark TEOS(0) gel) and examining the spectral response of the polysilicate phase alone. Figure 5 displays the resulting spectra that are dominated by the previously discussed asymmetric stretching of silica and silanol groups. However, there is another peak present at ca. 1165 cm^{-1} in all five of the spectra that is not immediately discernible in Figure 2, but is commonly observed in the spectra of gel-derived silica. There is, however, some ambiguity surrounding its origin in that this peak/shoulder has been attributed to both the 3-fold degenerate stretching frequencies of SiO_4 tetrahedron and the longitudinal optic mode of the asymmetric Si—O—Si stretch.[37,38] Regardless, it is a common characteristic of silica. The fact that all three significant peaks associated with silica are observable at the proper locations lends credence to the subtraction and ATR technique used in this study. Unfortunately, one artifact of the subtraction does become visible as the exposure time increases. This artifact is the ether linkage of the PTMO at 1100 cm^{-1}, which becomes more visible as the polysilicate at the surface of the sample begins to dissolve away.

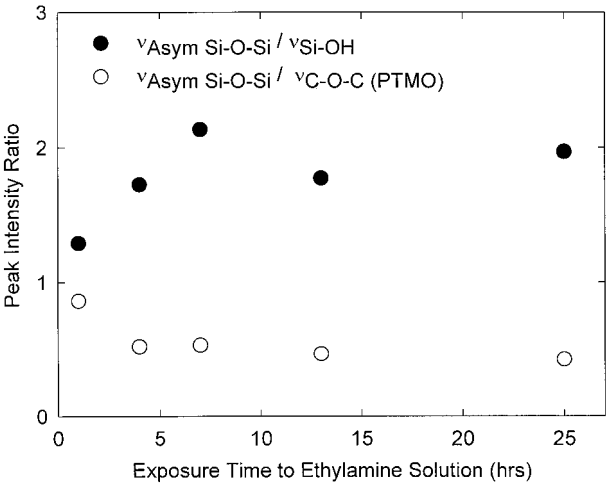

Figure 4 The ratio of peak intensities for the asymmetric Si—O—Si and Si—OH stretches (1050/955 cm^{-1}), as well as the ether linkage of the PTMO and Si—OH stretch (1100/955 cm^{-1}).

Returning to an analysis of the nature of the polysilicate phase, a technique has been developed by Mauritz and coworkers[41] on similar hybrid systems using the ratio of $\upsilon_{\text{Assym Si—O—Si}}$/

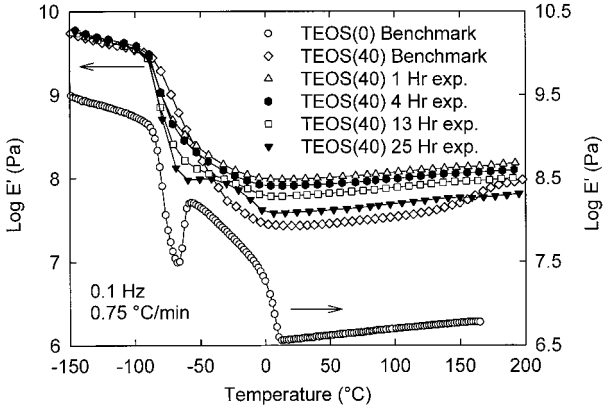

Figure 6 Dynamic mechanical storage modulus, E', as a function of temperature for the indicated gels. Note the different storage modulus range for the TEOS(0) gel, which was done to clearly show the crystallization observed.

υ_{Si-OH} (1050 cm^{-1}/955 cm^{-1}) as a semiquantitative/qualitative assessment of the degree of silica development present in hybrids.[42] This technique can be used on the gels in this study to examine the changes induced by the ethylamine processing. The ratio of these peaks as a function of the ethylamine exposure time are displayed as the upper plot in Figure 4 and reveal that at least 4 h is needed before there is an indiscernible change in the number of silanol species relative to oxygen bridged silicon atoms. Alternately stated, the first hour of exposure does not provide sufficient time for an equilibrium silicate structure to develop within the hybrid. Beyond this first hour, during which much of the absorption leading to equilibrium solvent uptake occurs, it seems that the silicate phase experiences no further change in its degree of condensation. A similar trend is observed in Figure 3, in that after the first hour of exposure, the number of the silanol species present, as evidenced by the area under the absorbance at ca. 3300 cm^{-1}, seems to remain unchanged and approximates the number present in the benchmark TEOS(0) gel.

To summarize the results of the ATR FTIR analysis, it seems that increased connectivity of the polysilicate phase is occurring at the surface of the gels. Based on the previously discussed changes in density, percent residue on ignition and DMS results presented in the next section, these changes are most certainly occurring throughout the bulk of the gel as well. In addition, some dissolution is taking place at the surface of the sample. However, this amount of loss is negligible and undoubtedly has little influence on the bulk properties of the gels. It is also apparent that an alternative to the FTIR analysis is solid-state Si^{29} NMR. NMR studies would confirm the structural changes of the silicate phase in the bulk of the material. As a result of recent funding, a new solid-state NMR will be available, and hence these studies will be possible in the near future.

Dynamic Mechanical Spectroscopy and Estimation of $\bar{M}_c$

The dynamic mechanical storage modulus, E', of the benchmark TEOS(0) and TEOS(40) gels, as well as the TEOS(40) gels that have been exposed to the ethylamine in water solution for up to 25 h appear in Figure 6. The features of interest include the glass to rubber transition, T_g, at ca. −80°C for all of the gels and the presence of crystallization in both the TEOS(0) gels [i.e., sharp increase in E' at ca. −70°C] and the TEOS(40) gels exposed to ethylamine for 25 h (i.e., plateau in E' extending from ca. −70°C to ca. 0°C). This onset of crystallization is evidence of increased phase separation induced by the ripening process. At temperatures greater than the T_g and above the crystalline melting point, the rubbery regimes of the TEOS(0) gel and ethylamine-exposed TEOS(40) gels exhibit significant linearity with increasing temperature, prompting the analysis developed in the Introduction. In addition, there is a region between ca. 30°C and 130°C where the benchmark TEOS(40) gel exhibits appreciable

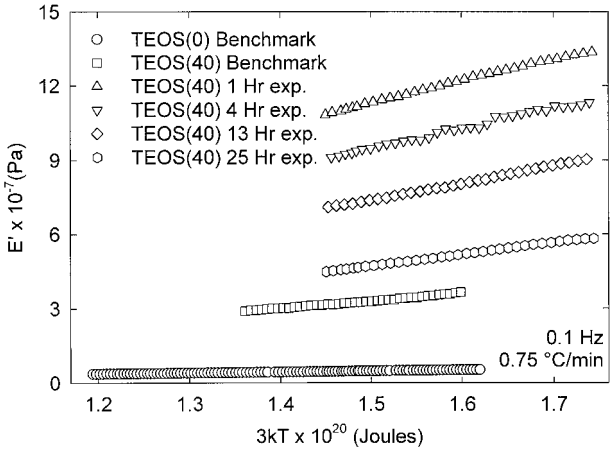

Figure 7 The rubbery regime of the gels investigated is expressed in terms of thermal energy. The slope of each line is the number of elastically active network chains per unit volume, N_v.

Table II Number of Elastically Active Network Chains Per Unit Volume at Each Frequency Measured Using the Dynamic Mechanical Spectrometer

	Test Frequency (Hz)					
Gel Type	0.1	0.5	1	2	5	10
TEOS(0) benchmark	0.40	—	0.39	—	—	0.39
TEOS(40) benchmark	2.99	2.90	2.86	2.85	2.74	2.65
TEOS(40) 1-h exposure	8.84	8.79	8.77	8.75	8.67	8.53
TEOS(40) 4-h exposure	8.05	8.03	8.00	7.91	7.86	7.80
TEOS(40) 13-h exposure	6.98	7.02	6.99	7.01	6.99	6.86
TEOS(40) 25-h exposure	4.75	4.77	4.74	4.73	4.68	4.60

linearity. The first equality in eq. (3) necessitates a plot of E' *vs.* 3 kT in the rubbery regime for a determination of the average number of elastically active network chains per unit volume. This data is displayed in Figure 7, where differences in slopes are observable. Although only the 0.1 Hz data is shown, Table II displays the slopes, $\bar{N}_v$, for all frequencies investigated. The exceptional linearity is confirmed in that the regression coefficients, r^2, for all gels and frequencies ranged from 0.995 to 0.998. Assuming tetrafunctional junctions, then the crosslink density is equal to $\bar{N}_v/2$. A review of the frequency dependence of $\bar{N}_v$ in Table II reveals that, as the test frequency increases, there are fewer chains contributing to the elastic force. This trend will be discussed in more detail.

The average molar mass between crosslinks can be calculated from the second equality in eq. (3) and the density values given in Table I. Figure 8 displays the estimated $\bar{M}_c$ values as a function of frequency. Recalling that the molar mass of the PTMO before triethoxysilane functionalization is ca. 2000 g mol^{-1}, values in the range of 1550–1600 g mol^{-1} for the TEOS(0) gels are promising. This is especially true, given that estimations of polysilicate volume percent based on molar mass variations upon curing and additive volumes indicate that ca. 4% by volume of polysilicate exists within the TEOS(0) gel, assuming a 75% conversion of ethoxysilane species to oxygen bridging SiO_4 tetrahedron. As expected, as the volume of polysilicate increases to 19% for the TEOS(40) gels, the average molar mass between crosslinks decreases to a range of 230–260 g mol^{-1}. Both the TEOS(0) and TEOS(40) benchmark gels, both with the potential for thermally induced ripening, exhibit an increase in $\bar{M}_c$ with increasing frequency. However, less significant increases are observable for the TEOS(40) ethylamine-exposed gels, which were just shown to possess chemically stable polysilicate phases. In addition, the values for $\bar{M}_c$ are significantly reduced for the ethylamine-exposed gels, with a minimum value of approximately 75 g mol^{-1} exhibited for the gels exposed for 1 h. As the exposure time increases to a maximum of 25 h, the value of $\bar{M}_c$ increases, reaching a maximum of ca. 145 g mol^{-1} for the 25-h exposure gels.

A reduction in the average molar mass between crosslinks is to be anticipated based on the incorporation of the anelastic (from the standpoint of entropy-driven polymer elasticity) polysilicate phase. For the sake of comparison, if only the vol-

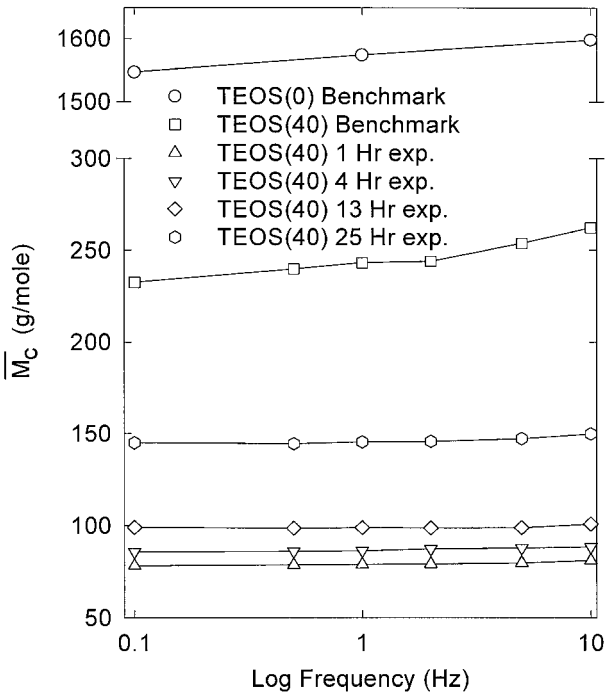

Figure 8 Frequency dependence of the average molar mass between crosslinks, $\bar{M}_c$, for the indicated gels.

ume fraction of PTMO is assumed elastic, then a rule of mixtures predicts that $\bar{M}_c$ values of 1920 g mol^{-1} and 1620 g mol^{-1} should be observed for the TEOS(0) and TEOS(40) gels, respectively, regardless of ethylamine exposure, because the total mass percent of polysilicate remains unchanged for all exposure times investigated (Table I). Because these values are much greater than those predicted from eq. (3) and displayed in Figure 8, the employment of rubber elasticity theory reveals that the near molecular level of mixing in these acid-catalyzed gels gives rise to restrictions of the PTMO chains by the polysilicate chains. Furthermore, the ripening induced by the ethylamine treatment does indeed result in phase sharpening, as evidenced by the increasing average chain length between crosslinks with increasing exposure time. This interaction-based analysis completely explains the mechanical, dynamic mechanical, density, and swelling response previously observed for these gels.[27] Another question remains, however, regarding the accuracy of the measured values, especially considering the use of "dynamic" moduli data and the possible chemical curing contributions known to be operative in the as-cast (0 hr) and 1-h exposed samples. It has also been shown previously that the increase of E', of the benchmark gels, is characteristic of "curing" in the gel structure.[11] Therefore, to validate further the values calculated from eq. (3), equilibrium swelling measurements were made with the goal of using eq. (5) to predict $\bar{M}_c$ values for the same gels.

Estimation of $\bar{M}_c$ via Equilibrium Swelling

Equation (5) necessitates knowledge of the volume fraction of polymer in the swollen state, v_{2m}, and the Flory-Huggins interaction parameter, $\chi_{1,2}$, for the given polymer–solvent–temperature combination used. With regard to the former values, equilibrium mass uptake of THF for the TEOS(40) and ethylamine-exposed TEOS(40) gels was measured at room temperature and the volume fraction of polymer calculated using eq. (6). The results are displayed in Figure 9 as a function of ethylamine solution exposure. Consistent with results predicted from the above analysis, as the benchmark TEOS(40) possess the greatest average molar mass between crosslinks, it swells the most and consequently has the lowest v_{2m} value. The gel exposed for 1 h had the lowest value of $\bar{M}_c$ and therefore swells the least and has the largest v_{2m} value. Continued exposure to the ethylamine induces phase separation and frees the previously restrained PTMO chains, thereby increasing $\bar{M}_c$, and allowing more swelling and decreasing v_{2m} values.

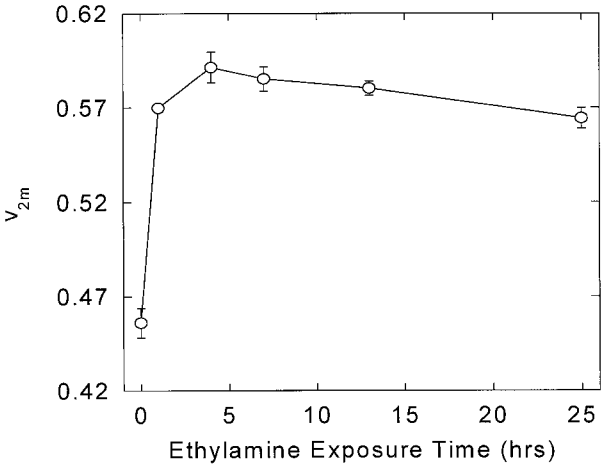

Figure 9 Values of the equilibrium volume fraction of polymer present in the swollen network, v_{2m}, for TEOS(40) gels as a function of ethylamine solution exposure time.

Determination of the Flory-Huggins interaction parameter for such a complex composite system necessitates an experimental estimate. Previous measurements of the solubility parameter for the TEOS(40)-based systems have been made by swelling the gel in solvents of differing Hildebrand parameters and using the maximum in the gel swelling coefficient (19.1 MPa$^{1/2}$) as an estimate of the Hildebrand parameter of the gels.[28] Using equation (7) and knowing that THF has a Hildebrand parameter of 18.6 MPa$^{1/2}$ and molar volume of 8.11×10^{-5} m^3 mol^{-1}, $\chi_{1,2}$ is calculated to be 0.0082. The exceptionally low value is not unreasonable, considering the affinity the PTMO should have for THF because the polymer is made from the ring-opening polymerization of this solvent. A concern arises regarding the incorporation of the lattice constant of entropic origin that some authors have put forth requiring that an additional value of ca. 0.34 be added to the $\chi_{1,2}$ value calculated using eq. (7).[34] For the sake of comparison, calculations of $\bar{M}_c$ using swelling were performed using both a $\chi_{1,2}$ of 0.0082 and 0.3482. These results are displayed in Figure 10, along with the values of $\bar{M}_c$ calculated using the 0.1 and 10 Hz DMS data from Figure 8. The overall good agreement between the two techniques is very encouraging, considering the ease with which the "dynamic" technique can be accomplished relative

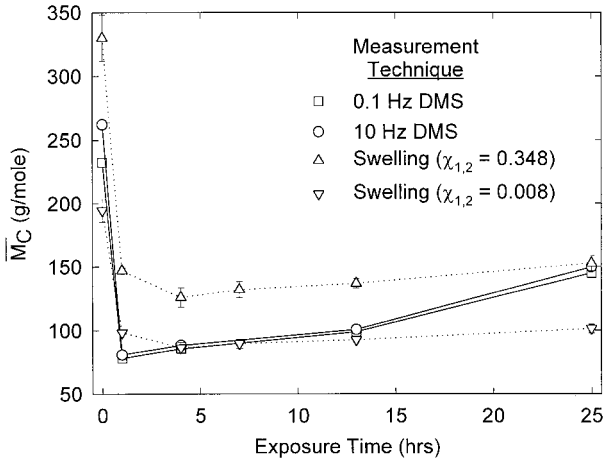

Figure 10 Comparison of the values for $\bar{M}_c$ calculated using eqs. (5)–(7) based on equilibrium swelling for both values of $\chi_{1,2}$ estimated, as well as values for $\bar{M}_c$ obtained using eqs. (4) and (5) for the 0.1 and 10 Hz data from the DMS.

to the various swelling experiments. The choice of the Hildebrand parameter is of obvious importance, and a value neglecting the entropic-derived 0.34 contribution seems to fit best over most of the range, with the exception being the gels with a 25-h exposure time to ethylamine solution.

CONCLUSIONS

DMS was performed on polysilicate crosslinked PTMO-based gels containing an estimated 4 and 19% by volume polysilicate. In addition, DMS was performed on samples of the 19% polysilicate gel that had been exposed to a basic ethylamine and water solution for times ranging from 0 to 25 h. The data revealed exceptional linearity in the storage modulus versus temperature plots warranting the use of elementary rubber elasticity theory as a tool for measuring the average molar mass between crosslinks. FTIR analysis revealed that, although some chemical change occurred during the first hour of exposure, discrediting the predicted values of $\bar{M}_c$, continued exposure resulted in equilibrium polysilicate structures. The significantly reduced values of $\bar{M}_c$ obtained using the DMS-based technique relative to those predicted by a rule of mixture for both the benchmark and ethylamine-exposed TEOS(40) gels confirm extensive interaction between the vitreous polysilicate phase and elastomeric PTMO phase. Furthermore, the increase in $\bar{M}_c$ with increasing exposure times to ethylamine is in good agreement with the onset of phase separation observable in the DMS data. Most interestingly, both the trends observed for the ethylamine-exposed gels and the magnitude of the values of $\bar{M}_c$ calculated were confirmed using equilibrium swelling calculations in conjunction with the Flory-Rehner equation. This excellent agreement suggests that elementary rubber elasticity theory is a good tool for investigating the extent of phase interaction occurring in these hybrid composites and that DMS provides a valid basis for the collection of data necessary for estimation of network parameters.

This work was supported in part by a duPont Young Faculty Investigator Award. In addition, insightful discussions with G. L. Wilkes are sincerely appreciated.

REFERENCES

1. A. B. Brennan and T. M. Miller, in *Kirk-Othmer Encyclopedia of Chemical Technology,* Vol. 12, 4th ed., John Wiley and Sons, Inc., New York, 1994, p. 644.
2. J. Wen and G. L. Wilkes, *Chem. Mater.,* **8,** 1667 (1996).
3. J. E. Mark, Y. P. Ningand, C. J. Jiang, and M. Y. Tang, *Polymer,* **26,** 2069 (1985).
4. G. B. Sohoni and J. E. Mark, *J. Appl. Polym. Sci.,* **45,** 1763 (1992).
5. H. H. Huang, B. Orler, and G. L. Wilkes, *Macromolecules,* **20,** 1322 (1987).
6. F. Surivet, T. M. Lam, J. P. Pascault, and C. Mai, *Macromolecules,* **25,** 5742 (1992).
7. H.-H. Huang, R. H. Glaser, and G. L. Wilkes, in *Inorganic and Organometallic Polymers,* ACS Symposium Series 360, American Chemical Society, Washington, DC, 1987, p. 355.
8. A. B. Brennan and G. L. Wilkes, *Polymer,* **32,** 733 (1991).
9. D. E. Rodrigues, A. B. Brennan, C. Betrabet, B. W. Wang, and G. L. Wilkes, *Chem. Mater.,* **4,** 1437 (1992).
10. J. L. W. Noell, G. L. Wilkes, D. K. Mohanty, and J. E. McGrath, *J. Appl. Polym. Sci.,* **40,** 1177 (1990).
11. A. B. Brennan, Ph.D. dissertation, Virginia Polytechnic Institute and State University, Blacksburg, VA, 1990.
12. A. Okada, *Polym. Prep., Am. Chem. Soc. Div. Polym. Chem.,* **28,** 447 (1987).
13. D. Tian, Ph. Dubois, and R. Jerome, *Polymer,* **37,** 3983 (1996).
14. C. J. Wung, Y. Pang, P. N. Prasad, and F. E. Karasz, *Polymer,* **32,** 605 (1991).
15. C. J. T. Landry, B. K. Coltrain, J. A. Wesson, N.

Zumbulyadis, and J. L. Lippert, *Polymer,* **33,** 1496 (1992).
16. C. J. T. Landry, B. K. Coltrain, and B. K. Brady, *Polymer,* **33,** 1486 (1992).
17. M. Toki, T. Y. Chow, T. Ohnaka, H. Samura, and T. Saegusa, *Polym. Bull.,* **29,** 653 (1992).
18. B. M. Novak and M. W. Ellsworth, *Mater. Sci. Eng.,* **A162,** 257 (1993).
19. P. Bosch, F. Del Monte, J. L. Mateo, and D. Levy, *J. Polym. Sci.: Poly. Chem.,* **34,** 3289 (1996).
20. C. L. Jackson, B. J. Bauer, A. I. Nakatani, and J. D. Barnes, *Chem. Mater.,* **8,** 727 (1996).
21. B. J. Bauer, D.-W. Liu, C. L. Jackson, and J. D. Barnes, *Polym. Adv. Tech.,* **7,** 333 (1995).
22. K. A. Mauritz, J. D. Stefanithis, S. V. Davis, R. W. Sheetz, R. K. Pope, G. L. Wilkes, and H.-H. Huang, *J. Appl. Polym. Sci.,* **55,** 181 (1995).
23. E. P. Giannelis, *Adv. Mater.,* **8,** 29 (1996).
24. K. J. Becker, J. A. Jensen, and A. Lukas III, U.S. Pat. 5,612,414 (1997).
25. T. M. Keller and D. Y. Son, U.S. Pat. 5,563,181 (1996).
26. K. G. Sharp and M. J. Michalczyk, U.S. Pat. 5,548,051 (1996).
27. A. B. Brennan and T. M. Miller, *Chem. Mater.,* **6,** 262 (1994).
28. A. B. Brennan, T. M. Miller, and R. V. Vinocur, in *Hybrid Organic-Inorganic Composites,* J. E. Mark, C. Y.-C. Lee, and P. A. Bianconi, Eds., ACS Symposium Series 585, American Chemical Society, Washington, DC, 1995, p. 142.
29. A. B. Brennan and T. M. Miller, in *Better Ceramics Through Chemistry VII: Organic / Inorganic Hybrid Materials,* B. K. Coltrain, C. Sanchez, D. W. Schaefer, and G. L. Wilkes, Eds., Mater. Res. Soc. Symp. Proc. Vol. 435, Materials Research Society, Pittsburgh, PA, 1996, p. 155.
30. R. K. Iler, *The Chemistry of Silica,* John Wiley & Sons, Inc., New York, 1979, p. 40.
31. G. L. Wilkes, *Polymer Science and Technology: An Interdisciplinary Approach; Part II Physical Aspects of Polymers,* American Chemical Society, Washington, DC, 1978, p. 129.
32. P. J. Flory, *Principles of Polymer Chemistry,* Cornell University Press, Ithaca, NY, 1953, p. 576.
33. P. J. Flory, *J. Chem. Phys.,* **18,** 108 (1950).
34. G. M. Bristow and W. F. Watson, *Trans. Farad. Soc.,* **54,** 1731 (1958).
35. R. H. Glaser, G. L. Wilkes, and C. E. Bronniman, *J. Non-Cryst. Solids,* **113,** 73 (1989).
36. R. M. Almeida and C. G. Pantano, *J. Appl. Phys.,* **68,** 4225 (1990).
37. D. L. Wood and E. M. Rabinovich, *Appl. Spec.,* **43,** 263 (1989).
38. A. Bertoluzza, C. Fagnano, M. A. Morelli, V. Gottardi, and M. Guglielmi, *J. Non-Cryst. Solids,* **48,** 117 (1982).
39. H. Yoshino, K. Kamiya, and H. Nasu, *J. Non-Cryst. Solids,* **126,** 68 (1990).
40. N. J. Harrick, *Internal Reflection Spectroscopy,* Wiley-Interscience, New York, 1967.
41. K. A. Mauritz, R. F. Storey, and C. K. Jones, in *Multiphase Polymer Materials: Blends, Ionomers and Interpenetrating Networks,* L. A. Ultracki and R. A. Weiss, Eds., ACS Symposium Series, American Chemical Society, Washington, DC, 1989, p. 401.
42. R. V. Gummaraju, R. B. Moore, and K. A. Mauritz, *J. Polym. Sci.: Polym. Phys.,* **34,** 2383 (1996).